PALEOCEANOGRAPHY, VOL. 8, NO. 5, PAGES 567-586, OCTOBER 1993

PALEOCEANOGRAPHY AND THE DIACHRONY OF RADIOLARIAN EVENTS IN THE EASTERN EQUATORIAL PACIFIC

T. C. Moore, Jr.
Department of Geological Sciences, University of Michigan, Ann Arbor

N. J. Shackleton
Subdepartment of Quaternary Research, University of Cambridge, Cambridge, England

N. G. Pisias
College of Oceanography, Oregon State University, Corvallis

Abstract. The development of an orbitally tuned time scale for the ODP leg 138 sites provides biostratigraphers a very high resolution chronostratigraphic framework. With this framework we are better able to define which of the first and last appearances of species appear to be synchronous. In addition, the geographic distribution of sites provides the means with which the detailed spatial patterns of invasion of new species and the extinction of older species can be mapped. These maps not only provide information on the process of evolution, migration, and extinction, they can also be related to water mass distributions and near-surface circulation of the ocean. Of 39 radiolarian events studied at 11 sites in the eastern equatorial Pacific, 28 were found to have a minimum range in their estimated age that exceeded 0.15 m.y. The temporal pattern of first and last appearances of these diachronous events have coherent spatial patterns that indicate shifts in the areas of high oceanographic gradients over the past 10 Ma. These changes in the locations of high gradient regions suggest that the South Equatorial Current (SEC) was north of its present position prior to approximately 7 Ma. There was a southward shift in the northern boundary of this current between approximately 6 and 7 Ma, and the development of a relatively strong gradient between the northeastern and northwestern sites. Between approximately 3.7 and 3.4 Ma, there was a very slight northward shift in the northern boundary of the SEC and the steep gradients between the northeastern and northwestern sites may have disappeared. This change is thought to be associated with the closing of the Isthmus of Panama. The temporal-spatial patterns of diachronous events younger than 3.4 Ma are consistent with patterns of circulation in the modern ocean.

Paper number 93PA01328.
0883-8305/93/93PA-01328$10.00

INTRODUCTION

There is a general belief held by biostratigraphers that some (but not all) first and last appearances of planktonic microfossils species are synchronous within broad regions of the oceans. In areas of the ocean where good chronostratigraphy has been provided by paleomagnetically dated cores, the degree of synchrony for radiolarians has been shown to be within approximately 0.2 m.y. [Hays et al., 1969; Hays, 1970, 1971; Johnson and Knoll, 1975; Theyer et al., 1978; Johnson and Wick, 1982; Johnson and Nigrini, 1985; Johnson et al., 1989; Caulet et al., 1993], and in cores having oxygen isotope stratigraphy as well, the degree of synchrony for some radiolarian species is even more tightly constrained [Hays and Shackleton, 1976; Alexandrovich, 1992]. In their far reaching studies of radiolarian stratigraphies these investigators have indicated, however, that the first and last appearances of many radiolarian species can be diachronous within one oceanographic zone (i.e., the tropical oceans) and even within individual ocean basins (i.e., the tropical Pacific and Indian oceans). In those parts of the ocean where biostratigraphic events have not been tightly tied to the paleomagnetic time scale, the dating of a section based solely on biostratigraphy is generally thought to be accurate to within approximately 0.5 m.y.

With the advent of orbitally tuned time scales we can go far beyond this degree of accuracy. Biostratigraphy still provides checks on the interpretation of magnetic reversal stratigraphy and on the process by which more continuous geochemical, lithologic, and biotic records are tuned to the calculated Milankovitch periods of orbital variation [Dowsett, 1989]. However, the need to use biostratigraphic first and last appearances as the sole means of establishing a chronostratigraphy is slowly fading. In this study we take the opportunity to use the high-resolution, orbitally tuned time scales as a tool to study the true nature of first appearances, evolution, and extinctions of planktonic species. Furthermore, the spatial coverage provided by the Ocean Drilling Program (ODP) sites which have complete recovery allow us to map the temporal patterns of the changing distribution of species as they develop in one region of the ocean, and through evolution, adaptation, or changing oceanographic conditions are able to migrate into other current systems and oceanographic regions [e.g., Dowsett, 1988, 1989; Kennett, 1970, 1978; Berggren et al., 1967].

The sites drilled on ODP leg 138 [Mayer et al., 1992] were successful in obtaining the most complete suite of cores yet recovered by ODP. One of the objectives of this cruise was to provide a network of complete stratigraphic sections with which the spatial and temporal history of Pacific equatorial circulation patterns could be reconstructed for the late Neogene. It can be demonstrated [Hagelberg et al., 1992] that we were remarkably successful in recovering all of the sections that were cored with the advanced piston corer (APC) and most of the sections cored with the extended core barrel (XCB). The successful recovery of these nearly complete, undisturbed sections, together with the highly detailed biostratigraphic, lithostratigraphic, and paleomagnetic studies conducted on these sections, provided us with the opportunity to produce an orbitally tuned time scale for these sites that goes back approximately 10 Ma [Shackleton et al., 1993]. With this time scale in hand we can then begin to investigate the true nature of biostratigraphic events. Within the chronostratigraphic framework developed by Shackleton et al. [1993] we will document the nature of first and last appearances of individual radiolarian species within the relatively small (but dynamic) region of the equatorial Pacific sampled by ODP leg 138.

METHODS

Radiolarian sample preparation, sampling record and stratigraphy are reported by Moore [1993]. At least three samples were taken from each core and examined on board to establish the radiolarian stratigraphy. One sample per core section (1.5 m) was taken in sites 853 and 854; however, radiolarians were absent from the interval older than late Pliocene at these two sites. Sites 845, 846, 848, and 852 were sampled after the cruise at the spacing necessary to assure that each radiolarian event in these sites was resolved to within 0.05 to 0.1 million years. Radiolarian events in the other sites are constrained solely by the samples taken on board. The average (and maximum) age resolution of events for all sites are given in Tables 1a-1f.

Radiolarian taxonomy is reported by Moore [1993]; however, it should be pointed out that taxonomic variation in radiolaria is comparatively large (relative to other marine microfossils), especially near the beginning and end of species ranges [Caulet et al., 1993]. These variations, when considered in both a geographical and temporal context, offer an opportunity for future studies to carefully examine the processes and rates of evolution. For this study, however, these variations may have caused errors in the definition of first and last appearances of individual species. Caulet et al. [1993] note morphologic variations or transitional forms in *Anthocyrtidium angulare, A. jenghisi, Theocorythium vetulum, T. trachelium, Lychnodictyum audax, Anthocyrtidium pliocenica,* and *Amphirhopalum ypsilon*. I have tended to use a rather strict definition of these species as defined in references cited by Moore [1993]; however, this does not necessarily preclude the unintentional inclusion of transitional forms - particularly for *Anthocyrtidium angulare, Theocorythium vetulum,* and *T. trachelium* (as described by Caulet et al. [1993]). What can be claimed is a site-to-site consistency in taxonomy of the species used.

The multiple holes drilled at each site on ODP leg 138 were correlated on board using GRAPE, color reflectance, and magnetic susceptibility data [Hagelberg et al., 1992]. This correlation produced a composite section for each site that demonstrates the completeness of recovery of the section at that site. The integration of biostratigraphy, lithostratigraphy, and paleomagnetic data provided both the means of detailed intersite correlation and the initial time scale [Shackleton et al., 1992]. This initial time scale together with the revised geomagnetic time scale of Cande and Kent [1992] provided the starting point for tuning the composite GRAPE records and the records of oxygen isotopes to the calculated orbital parameters [Berger and Loutre, 1991; Shackleton et al., 1993]. In the older part of the section presented here (6-10 Ma) the quality of the stratigraphic data used in the tuning deteriorates slightly and sedimentation rates decline [Shackleton et al., 1993]. Furthermore, Berger and Loutre [1991] do not claim accuracy for their astronomical reconstructions beyond approximately 5 Ma. However, there is good biostratigraphy, magnetostratigraphy and lithostratigraphy for most of the sites in this older part of the record. On the basis of these data and new radiometric ages, detailed inter-site correlations and at least a partially tuned age model have been developed [Shackleton et al., 1993]. Down to approximately 6 Ma, the tuned ages of individual paleomagnetic datums are within approxi-

TABLE 1a. Radiolarian Biostratigraphic Events, ODP Leg 138, Sites 844 and 845

	Events*	Types†	844					845				
			Depth (mcd)‡		Age, Ma		Md Age,§	Depth (mcd)‡		Age, Ma		Md Age,§
			Top	Bottom	Top	Bottom	Ma	Top	Bottom	Top	Bottom	Ma
T	*Stylatractus universus*	Sync	4.53	9.6	0.34	0.72	0.53	12.09	12.58	0.40	0.42	0.41
B	*Collosphaera tuberosa*	Sync	4.53	9.6	0.34	0.72	0.53	15.58	18.09	0.58	0.70	0.64
T	*Lamprocyrtis neoheteroporos*	Sync	11.43	12.73	0.93	1.08	1.01	24.47	25.06	1.02	1.05	1.04
T	*Anthocyrtidium angulare*	Sync*	11.43	12.73	0.93	1.08	1.01	25.06	25.97	1.05	1.10	1.08
T	*Theocorythium vetulum*	Sync	12.73	15.61	1.08	1.45	1.27	26.45	27.85	1.12	1.19	1.16
B	*Lamprocyrtis nigriniae*	NEC	12.73	15.61	1.08	1.45	1.27	27.85	29.53	1.19	1.28	1.24
B	*Theocorythium trachelium*	NECC	15.61	19.05	1.45	1.93	1.69	32.83	33.65	1.45	1.49	1.47
B	*Pterocorys minythorax*	NECC	15.61	19.05	1.45	1.93	1.69	33.65	35.83	1.49	1.60	1.54
T	*Pterocanium prismatium*	Sync	15.61	19.05	1.45	1.93	1.69	37.22	38.62	1.67	1.74	1.70
B	*Anthocyrtidium angulare*	Sync	15.61	19.05	1.45	1.93	1.69	38.62	39.81	1.74	1.80	1.77
T	*Lamprocyrtis heteroporos*	TROP	15.61	19.05	1.45	1.93	1.69	33.65	35.83	1.49	1.60	1.54
T	*Anthocyrtidium jenghisi*	NEC	20.35	22.05	2.21	2.57	2.39	43.71	46.71	2.03	2.33	2.18
B	*Theocalyptra davisiana*	Sync	22.05	23.35	2.57	2.94	2.76	49.6	51.93	2.62	2.86	2.74
T	*Stichocorys peregrina*	SEC, NEC	22.05	23.35	2.57	2.94	2.76	51.93	52.16	2.86	2.88	2.87
B	*Lamprocyrtis neoheteroporos*	PC	20.35	22.05	2.94	3.46	3.20	55.37	56.18	3.10	3.17	3.14
B	*Lamprocyrtis heteroporos*	PC	23.35	24.93	2.94	3.46	3.20	54.58	55.37	3.10	3.17	3.14
T	*Anthocyrtidium pliocenica*	ED, PC	23.35	24.93	2.94	3.46	3.20	56.78	59.72	3.29	3.59	3.44
B	*Amphirhopalum ypsilon*	NECC	24.93	26.05	3.46	3.84	3.65	59.72	60.17	3.59	3.64	3.62
T	*Lychnodictyum audax*	TROP	26.05	31.01	3.84	5.18	4.51	63.36	64.06	3.97	4.04	4.00
T	*Phormostichoartus fistula*	NECC	31.01	31.70	5.18	5.30	5.24	56.78	59.72	3.29	3.56	3.44
B	*Spongaster tetras*	Sync*	24.93	26.05	3.46	3.84	3.65	61.76	62.56	3.97	4.04	4.00
T	*Didymocyrtis penultima*	Sync*	26.05	31.01	3.84	5.18	4.51	71.11	71.9	4.74	4.85	4.79
T	*Phormostichoartus doliolum*	SEC	26.05	31.01	3.84	5.18	4.51	63.36	64.06	3.97	4.04	4.00
B	*Pterocanium prismatium*	Sync*	24.93	26.05	3.46	3.84	3.65	66.7	67.06	4.33	4.36	4.34
B	*Theocorythium vetulum*	NECC	31.7	33.2	5.30	5.55	5.43	77.15	78	5.30	5.35	5.32
T	*Solenosphaera omnitubus*	TROP	33.20	34.70	5.55	5.81	5.68	77.15	78	5.30	5.35	5.32
T	*Siphostichartus corona*	SEC	34.70	40.75	5.81	6.88	6.35	103	104.2	7.06	7.14	7.10
T	*Stichocorys johnsoni*	TROP	34.70	40.75	5.81	6.88	6.35	94.98	96.18	6.44	6.54	6.49
T	*Calocycletta caepa*	SEC	34.70	40.75	5.81	6.88	6.35	102.1	103	6.98	7.06	7.02
	S. delmontensis > S. peregrina	TROP	34.70	40.75	5.81	6.88	6.35	99.18	99.86	6.76	6.81	6.78
B	*Solenosphaera omnitubus*	TROP	42.33	43.75	7.20	7.47	7.34	104.2	105	7.14	7.20	7.17
T	*Diartus hughesi*	Sync	43.75	46.55	7.47	7.75	7.61	110.7	111.2	7.59	7.63	7.61
T	*Botryostrobus miralestensis*	TROP	46.55	50.70	7.75	8.15	7.95	121	121.7	8.21	8.25	8.23
T	*Diartus petterssoni*	SEC	50.70	52.60	8.15	8.45	8.30	128.8	129.7	8.59	8.63	8.61
	D. petterssoni > D. hughesi	Sync	53.70	56.62	8.63	8.93	8.78	130.6	131.8	8.63	8.67	8.65

TABLE 1a. (continued)

Events*	Types†	844					845				
		Depth (mcd)‡		Age, Ma		Md Age,§	Depth (mcd)‡		Age, Ma		Md Age,§
		Top	Bottom	Top	Bottom	Ma	Top	Bottom	Top	Bottom	Ma
B *Stichocorys johnsoni*	NECC	56.62	62.80	8.93	9.67	9.30	130.6	131.8	8.67	8.72	8.70
T *Stichocorys wolffii*	Sync	53.70	56.62	8.53	8.93	8.73	133.4	134.7	8.80	8.85	8.83
T *Cyrtocapsella japonica*	Sync	65.80	68.76	9.91	10.20	10.04	154.1	154.8	10.06	10.11	10.08
T *Carpocanopsis cristata*	NECC	68.76	72.75	10.20	10.50	10.35	158.5	160.5	10.37	10.52	10.45

* T, last appearance; B, first appearance.

† "Type" denotes the Synchronous (Sync) and Diachronous events. An asterisk by the designation "Sync*" is given if the data from sites 844 and 845 are not considered in categorizing the event type. For the diachronous events the water mass or current system in which the first appearances appear the oldest and the last appearances appear the youngest are given under the heading "Type": ED, equatorial divergence; NEC, North Equatorial Current; NECC, North Equatorial Counter Current; PC, Peru Current extension; SEC, South Equatorial Current; Trop, Tropical water mass (north and south of the equatorial divergence - Peru Current extension).

‡ Here mcd is meters composite depth as used by Mayer et al. [1992].

§ The given median age is used (Figures 5-18).

TABLE 1b. Radiolarian Biostratigraphic Events, ODP Leg 138, Sites 846 and 847

Events*	Types†	846					847				
		Depth (mcd)‡		Age, Ma		Md Age,§	Depth (mcd)‡		Age, Ma		Md Age,§
		Top	Bottom	Top	Bottom	Ma	Top	Bottom	Top	Bottom	Ma
T *Stylatractus universus*	Sync	14.70	16.10	0.39	0.42	0.40	13.73	16.21	0.41	0.49	0.45
B *Collosphaera tuberosa*	Sync	17.49	22.65	0.45	0.61	0.53	18.34	20.45	0.58	0.65	0.62
T *Lamprocyrtis neoheteroporos*	Sync	36.25	38.04	0.99	1.05	1.02	32.43	33.47	1.07	1.09	1.08
T *Anthocyrtidium angulare*	Sync*	40.90	42.40	1.12	1.15	1.13	33.47	35.43	1.09	1.15	1.12
T *Theocorythium vetulum*	Sync	44.80	45.99	1.22	1.28	1.25	38.41	39.5	1.22	1.26	1.24
B *Lamprocyrtis nigriniae*	NEC	44.80	45.99	1.22	1.28	1.25	35.43	38.41	1.15	1.22	1.19
B *Theocorythium trachelium*	NECC	57.00	58.60	1.60	1.65	1.63	47.89	49.08	1.50	1.54	1.52
B *Pterocorys minythorax*	NECC	53.50	54.74	1.49	1.52	1.51	49.08	53.68	1.54	1.70	1.62
T *Pterocanium prismatium*	Sync	60.44	65.59	1.69	1.82	1.76	54.59	56.68	1.71	1.78	1.75
B *Anthocyrtidium angulare*	Sync	60.44	65.59	1.69	1.82	1.76	54.59	56.68	1.71	1.78	1.75
T *Lamprocyrtis heteroporos*	TROP	77.90	79.20	2.07	2.09	2.08	67.85	70.84	2.04	2.13	2.08
T *Anthocyrtidium jenghisi*	NEC	89.15	90.75	2.35	2.39	2.37	81.01	86.58	2.45	2.61	2.53
B *Theocalyptra davisiana*	Sync	105.78	110.10	2.71	2.80	2.76	89.58	91.95	2.71	2.79	2.75

TABLE 1b. (continued)

Events*	Types†	846 Depth (mcd)‡ Top	846 Depth (mcd)‡ Bottom	846 Age, Ma Top	846 Age, Ma Bottom	846 Md Age,§ Ma	847 Depth (mcd)‡ Top	847 Depth (mcd)‡ Bottom	847 Age, Ma Top	847 Age, Ma Bottom	847 Md Age,§ Ma
T *Stichocorys peregrina*	SEC, NEC	105.78	110.10	2.71	2.80	2.76	91.95	92.58	2.79	2.80	2.80
B *Lamprocyrtis neoheteroporos*	PC	135.45	136.45	3.35	3.37	3.36	97.98	99.83	3.34	3.36	3.35
B *Lamprocyrtis heteroporos*	PC	132.45	133.45	3.42	3.44	3.43	108.3	109	3.34	3.36	3.35
T *Anthocyrtidium pliocenica*	ED, PC	129.41	130.45	3.30	3.35	3.33	103.98	108.3	3.20	3.34	3.27
B *Amphirhopalum ypsilon*	NECC	145.15	147.93	3.65	3.75	3.70	124.61	128.74	3.92	4.09	4.01
T *Lychnodictyum audax*	TROP	155.70	157.70	3.99	4.04	4.02	114.46	119.03	3.56	3.71	3.64
T *Phormostichoartus fistula*	NECC	165.70	167.20	4.31	4.34	4.32	128.74	129	4.09	4.11	4.10
B *Spongaster tetras*	Sync*	157.70	160.32	4.04	4.13	4.09	129	132	4.11	4.23	4.17
T *Didymocyrtis penultima*	Sync*	160.32	161.80	4.13	4.18	4.16	129	132	4.11	4.23	4.17
T *Phormostichoartus doliolum*	SEC	157.70	160.32	4.04	4.13	4.09	128.74	129	4.09	4.11	4.10
B *Pterocanium prismatium*	Sync*	183.65	184.41	4.72	4.73	4.73	160.45	163.45	4.83	4.87	4.85
B *Theocorythium vetulum*	NECC	187.85	191.02	4.81	4.89	4.85	163.45	165.43	4.87	4.89	4.88
T *Solenosphaera omnitubus*	TROP	209.70	214.10	5.38	5.47	5.43	184.54	188.35	5.37	5.48	5.42
T *Siphostichartus corona*	SEC	215.60	216.89	5.50	5.53	5.52	197.35	200.35	5.66	5.76	5.71
T *Stichocorys johnsoni*	TROP	263.41	265.10	6.42	6.49	6.46	236.35	239.35	6.42	6.48	6.45
T *Calocycletta caepa*	SEC	267.22	269.50	6.56	6.65	6.60	239.35	241.62	6.48	6.52	6.50
S. delmontensis > S. peregrina	TROP	267.22	270.71	6.56	6.70	6.63	236.35	245.35	6.42	6.59	6.50
B *Solenosphaera omnitubus*	TROP	288.66	290.20	7.26	7.32	7.29					
T *Diartus hughesi*	Sync	299.97	300.30	7.64	7.66	7.65					
T *Botryostrobus miralestensis*	TROP	312.10	315.10	8.37	8.59	8.48					
T *Diartus petterssoni*	SEC	312.10	315.10	8.37	8.59	8.48					
D. petterssoni > D. hughesi	Sync	315.10	317.20	8.59	8.75	8.67					
B *Stichocorys johnsoni*	NECC	315.10	317.20	8.59	8.72	8.65					
T *Stichocorys wolffii*	Sync	318.85	319.60	8.84	8.87	8.86					
T *Cyrtocapsella japonica*	Sync	338.90	340.40	10.03	10.15	10.09					
T *Carpocanopsis cristata*	NECC	348.52	349.99	10.78	10.84	10.81					

* T, last appearance; B, first appearance.

† "Type" denotes the Synchronous (Sync) and Diachronous events. An asterisk by the designation "Sync*" is given if the data from sites 844 and 845 are not considered in categorizing the event type. For the diachronous events the water mass or current system in which the first appearances appear the oldest and the last appearances appear the youngest are given under the heading "Type": ED, equatorial divergence; NEC, North Equatorial Current; NECC, North Equatorial Counter Current; PC, Peru Current extension; SEC, South Equatorial Current; Trop, Tropical water mass (north and south of the equatorial divergence - Peru Current extension).

‡ Here mcd is meters composite depth as used by Mayer et al. [1992].

§ The given median age is used (Figures 5-18).

TABLE 1c. Radiolarian Biostratigraphic Events, ODP Leg 138, Sites 848 and 849

Events*	Types†	848					849				
		Depth (mcd)‡		Age, Ma		Md Age,§	Depth (mcd)‡		Age, Ma		Md Age,§
		Top	Bottom	Top	Bottom	Ma	Top	Bottom	Top	Bottom	Ma
T *Stylatractus universus*	Sync	7.1	8.6	0.48	0.56	0.52	12.75	15.75	0.40	0.51	0.45
B *Collosphaera tuberosa*	Sync	9.74	10.02	0.63	0.65	0.64	17.58	24.35	0.58	0.85	0.72
T *Lamprocyrtis neoheteroporos*	Sync	17.75	18.25	1.09	1.12	1.10	27.35	29.26	0.96	1.04	1.00
T *Anthocyrtidium angulare*	Sync*	18.25	18.75	1.12	1.15	1.14	29.26	34.85	1.04	1.25	1.15
T *Theocorythium vetulum*	Sync	18.75	19.23	1.15	1.19	1.17	29.26	34.85	1.04	1.25	1.15
B *Lamprocyrtis nigriniae*	NEC	19.75	20.25	1.22	1.25	1.24	29.26	34.85	1.04	1.25	1.15
B *Theocorythium trachelium*	NECC	23.24	23.75	1.47	1.52	1.49	40.52	43.15	1.43	1.54	1.49
B *Pterocorys minythorax*	NECC	25.68	26.18	1.75	1.79	1.77	40.52	43.15	1.43	1.54	1.49
T *Pterocanium prismatium*	Sync	25.23	25.65	1.69	1.74	1.72	48.03	48.75	1.73	1.76	1.75
B *Anthocyrtidium angulare*	Sync	25.68	26.18	1.75	1.79	1.77	48.03	48.75	1.73	1.76	1.75
T *Lamprocyrtis heteroporos*	TROP	23.24	23.75	1.47	1.52	1.49	43.15	44.93	1.54	1.61	1.58
T *Anthocyrtidium jenghisi*	NEC	29.65	30.33	2.35	2.47	2.41	70.17	70.75	2.48	2.51	2.50
B *Theocalyptra davisiana*	Sync	31.35	31.86	2.64	2.71	2.67	73.71	78.5	2.62	2.81	2.72
T *Stichocorys peregrina*	SEC, NEC	31.35	31.86	2.64	2.71	2.67	73.71	78.5	2.62	2.81	2.72
B *Lamprocyrtis neoheteroporos*	PC	30.33	30.85	3.18	3.25	3.22	88.95	89.24	3.22	3.31	3.27
B *Lamprocyrtis heteroporos*	PC	34.36	34.66	3.18	3.25	3.22	89.24	91.95	3.22	3.31	3.27
T *Anthocyrtidium pliocenica*	ED, PC	36.45	36.85	3.59	3.66	3.63	89.24	91.95	3.22	3.31	3.27
B *Amphirhopalum ypsilon*	NECC	37.45	37.95	3.80	3.93	3.87	109.9	111.07	3.96	4.00	3.98
T *Lychnodictyum audax*	TROP	36.85	36.92	3.66	3.68	3.67	104.29	109.9	3.76	3.96	3.86
T *Phormostichoartus fistula*	NECC	36.85	36.92	3.66	3.68	3.67	102.66	104.29	3.69	3.76	3.73
B *Spongaster tetras*	Sync*	38.45	38.82	4.05	4.15	4.10	115.76	120.25	4.17	4.32	4.25
T *Didymocyrtis penultima*	Sync*	38.45	38.82	4.05	4.15	4.10	115.76	120.25	4.17	4.32	4.25
T *Phormostichoartus doliolum*	SEC	36.85	36.92	3.66	3.68	3.67	104.29	109.9	3.76	3.96	3.86
B *Pterocanium prismatium*	Sync*	44.42	44.95	4.75	4.79	4.77	142.22	143.16	4.74	4.75	4.75
B *Theocorythium vetulum*	NECC	46.48	47	4.90	4.95	4.93	143.16	153.7	4.75	5.00	4.88
T *Solenosphaera omnitubus*	TROP	47	47.5	4.95	4.99	4.97	176.75	179.75	5.39	5.42	5.41
T *Siphostichartus corona*	SEC	54.5	55.87	5.42	5.50	5.46	188.39	191.36	5.59	5.62	5.61
T *Stichocorys johnsoni*	TROP	67.35	67.85	6.30	6.35	6.32	237.8	242.79	6.23	6.33	6.28
T *Calocycletta caepa*	SEC	65.85	66.47	6.17	6.23	6.20	237.8	242.79	6.23	6.33	6.28
S. delmontensis > S. peregrina	TROP	70.75	70.81	6.57	6.84	6.70	274.1	275.55	6.61	6.68	6.65
B *Solenosphaera omnitubus*	TROP	76.77	81.41	7.06	7.45	7.26	284.19	286.76	6.97	7.07	7.02
T *Diartus hughesi*	Sync	81.8	82.4	7.51	7.65	7.58	306.2	308.78	7.62	7.84	7.73
T *Botryostrobus miralestensis*	TROP	84.35	84.85	8.02	8.20	8.11	318.17	324.05	8.21	8.35	8.28
T *Diartus petterssoni*	SEC	86.7	87.18	8.49	8.57	8.53	318.17	324.05	8.21	8.35	8.28
D. petterssoni > D. hughesi	Sync	88.18	88.85	8.72	8.82	8.77	327.57	329.74	8.53	8.62	8.58

TABLE 1c. (continued)

	Events*	Types†	848					849				
			Depth (mcd)‡		Age, Ma		Md Age,§	Depth (mcd)‡		Age, Ma		Md Age,§
			Top	Bottom	Top	Bottom	Ma	Top	Bottom	Top	Bottom	Ma
B	*Stichocorys johnsoni*	NECC	86.7	87.18	8.49	8.57	8.53	334.7	337.2	8.90	9.03	8.97
T	*Stichocorys wolffii*	Sync	88.85	89.35	8.82	8.89	8.86	334.7	337.2	8.90	9.03	8.97
T	*Cyrtocapsella japonica*	Sync						351.06	355.9	9.88	10.20	10.04
T	*Carpocanopsis cristata*	NECC						366.55	369.56	10.80	10.90	10.85

* T, last appearance; B, first appearance.

† "Type" denotes the Synchronous (Sync) and Diachronous events. An asterisk by the designation "Sync*" is given if the data from sites 844 and 845 are not considered in categorizing the event type. For the diachronous events the water mass or current system in which the first appearances appear the oldest and the last appearances appear the youngest are given under the heading "Type": ED, equatorial divergence; NEC, North Equatorial Current; NECC, North Equatorial Counter Current; PC, Peru Current extension; SEC, South Equatorial Current; Trop, Tropical water mass (north and south of the equatorial divergence - Peru Current extension).

‡ Here mcd is meters composite depth as used by Mayer et al. [1992].

§ The given median age is used (Figures 5-18).

TABLE 1d. Radiolarian Biostratigraphic Events, ODP Leg 138, Sites 850 and 851

	Events*	Types†	850					851				
			Depth (mcd)‡		Age, Ma		Md Age,§	Depth (mcd)‡		Age, Ma		Md Age,§
			Top	Bottom	Top	Bottom	Ma	Top	Bottom	Top	Bottom	Ma
T	*Stylatractus universus*	Sync	8.6	11.65	0.41	0.58	0.50	6.45	7.58	0.39	0.45	0.42
B	*Collosphaera tuberosa*	Sync	11.65	12.78	0.58	0.63	0.61	9.86	12.45	0.49	0.65	0.57
T	*Lamprocyrtis neoheteroporos*	Sync	20.02	23	1.00	1.13	1.07	21.5	22.69	1.11	1.18	1.15
T	*Anthocyrtidium angulare*	Sync*	20.02	23	1.00	1.13	1.07	22.69	23.75	1.18	1.25	1.22
T	*Theocorythium vetulum*	Sync	24.05	26.25	1.19	1.32	1.26	23.75	26.75	1.25	1.39	1.32
B	*Lamprocyrtis nigriniae*	NEC	24.05	26.25	1.19	1.32	1.26	22.69	23.75	1.18	1.25	1.22
B	*Theocorythium trachelium*	NECC	29.2	32.25	1.46	1.63	1.55	31.25	33.26	1.66	1.78	1.72
B	*Pterocorys minythorax*	NECC	32.25	33.39	1.63	1.70	1.67	31.25	33.26	1.66	1.78	1.72
T	*Pterocanium prismatium*	Sync	33.39	38.45	1.70	1.93	1.82	31.25	33.26	1.66	1.78	1.72
B	*Anthocyrtidium angulare*	Sync	33.39	38.45	1.70	1.93	1.82	31.25	33.26	1.66	1.78	1.72
T	*Lamprocyrtis heteroporos*	TROP	29.2	32.25	1.46	1.63	1.55	29.75	31.25	1.56	1.66	1.61
T	*Anthocyrtidium jenghisi*	NEC	50.01	51	2.45	2.52	2.49	41.81	44.5	2.27	2.37	2.32
B	*Theocalyptra davisiana*	Sync	54	55.48	2.65	2.73	2.69	50.9	52.19	2.73	2.77	2.75

TABLE 1d. (continued)

Events*	Types†	850					851				
		Depth (mcd)‡		Age, Ma		Md Age,§	Depth (mcd)‡		Age, Ma		Md Age,§
		Top	Bottom	Top	Bottom	Ma	Top	Bottom	Top	Bottom	Ma
T *Stichocorys peregrina*	SEC, NEC	55.48	58.6	2.73	2.86	2.80	50.9	52.19	2.73	2.77	2.75
B *Lamprocyrtis neoheteroporos*	PC	61.56	64.6	3.13	3.19	3.16	54.92	55.95	3.13	3.29	3.21
B *Lamprocyrtis heteroporos*	PC	64.6	66.1	3.13	3.19	3.16	58.95	61.95	3.13	3.29	3.21
T *Anthocyrtidium pliocenica*	ED, PC	64.6	66.1	3.13	3.19	3.16	63.45	65.21	3.37	3.45	3.41
B *Amphirhopalum ypsilon*	NECC	79.85	82.85	3.81	3.95	3.88	73.49	75.7	3.95	4.10	4.02
T *Lychnodictyum audax*	TROP	76.66	79.85	3.68	3.81	3.74	69.45	70.95	3.67	3.77	3.72
T *Phormostichoartus fistula*	NECC	72.15	76.66	3.48	3.68	3.58	65.21	66.45	3.45	3.52	3.48
B *Spongaster tetras*	Sync*	87.34	89.35	4.20	4.32	4.26	77	78.99	4.15	4.27	4.21
T *Didymocyrtis penultima*	Sync*	87.34	89.35	4.20	4.32	4.26	77	78.99	4.15	4.27	4.21
T *Phormostichoartus doliolum*	SEC	79.85	82.85	3.81	3.95	3.88	70.95	73.49	3.77	3.95	3.86
B *Pterocanium prismatium*	Sync*	108.35	111.35	4.76	4.84	4.80	84.44	94.54	4.51	4.88	4.69
B *Theocorythium vetulum*	NECC	134.49	140.15	5.39	5.52	5.46	108.75	111.75	5.38	5.45	5.42
T *Solenosphaera omnitubus*	TROP	133.47	134.49	5.36	5.39	5.38	108.75	111.75	5.38	5.45	5.42
T *Siphostichartus corona*	SEC	152.75	153.8	5.75	5.76	5.76	127.64	130.4	5.83	5.88	5.86
T *Stichocorys johnsoni*	TROP	190.55	191.7	6.31	6.36	6.34	148.52	150.38	6.25	6.28	6.26
T *Calocycletta caepa*	SEC	190.55	191.7	6.31	6.36	6.34	150.38	151.95	6.28	6.33	6.31
S. delmontensis > S. peregrina	TROP	220.58	223.15	6.65	6.72	6.68	176.2	179.2	6.63	6.68	6.66
B *Solenosphaera omnitubus*	TROP	239.7	242.45	7.12	7.17	7.14	183.37	190.85	6.80	7.01	6.91
T *Diartus hughesi*	Sync	261.35	264.35	7.71	7.78	7.75	208.78	217.65	7.52	7.72	7.62
T *Botryostrobus miralestensis*	TROP	278.01	283.65	8.19	8.35	8.27	233.25	236.2	8.13	8.27	8.20
T *Diartus petterssoni*	SEC	283.65	286.65	8.35	8.40	8.38	236.2	236.49	8.27	8.31	8.29
D. petterssoni > D. hughesi	Sync	293.25	297.32	8.59	8.72	8.66	246.64	254.65	8.57	8.82	8.70
B *Stichocorys johnsoni*	NECC	297.32	299.95	8.72	8.81	8.77	257.65	260.63	8.87	8.94	8.90
T *Stichocorys wolffii*	Sync	299.95	307.09	8.81	9.03	8.92	260.63	261.82	8.94	8.98	8.96
T *Cyrtocapsella japonica*	Sync	338.55	341.55	10.10	10.20	10.15	294.5	297.5	10.05	10.12	10.09
T *Carpocanopsis cristata*	NECC	360.85	363.85	10.60	10.70	10.65	321.04	324.6	10.64	10.72	10.68

* T, last appearance; B, first appearance.

† "Type" denotes the Synchronous (Sync) and Diachronous events. An asterisk by the designation "Sync*" is given if the data from sites 844 and 845 are not considered in categorizing the event type. For the diachronous events the water mass or current system in which the first appearances appear the oldest and the last appearances appear the youngest are given under the heading "Type": ED, equatorial divergence; NEC, North Equatorial Current; NECC, North Equatorial Counter Current; PC, Peru Current extension; SEC, South Equatorial Current; Trop, Tropical water mass (north and south of the equatorial divergence - Peru Current extension).

‡ Here mcd is meters composite depth as used by Mayer et al. [1992].

§ The given median age is used (Figures 5-18).

TABLE 1e. Radiolarian Biostratigraphic Events, ODP Leg 138, Sites 852 and 853

Events*	Types†	852					853				
		Depth (mcd)‡		Age, Ma		Md Age,§	Depth (mcd)‡		Age, Ma		Md Age,§
		Top	Bottom	Top	Bottom	Ma	Top	Bottom	Top	Bottom	Ma
T *Stylatractus universus*	Sync	4	4.59	0.39	0.45	0.42		<1.1			
B *Collosphaera tuberosa*	Sync	5.86	8.8	0.53	0.77	0.65		<1.1			
T *Lamprocyrtis neoheteroporos*	Sync	13.25	13.75	1.11	1.15	1.13	4.25	5.35	1.08	1.30	1.19
T *Anthocyrtidium angulare*	Sync*	13.25	13.75	1.11	1.15	1.13	4.25	5.35	1.08	1.30	1.19
T *Theocorythium vetulum*	Sync	14.25	14.75	1.21	1.24	1.22	4.25	5.35	1.08	1.30	1.19
B *Lamprocyrtis nigriniae*	NEC	14.25	14.75	1.21	1.24	1.22	5.35	6.85	1.30	1.59	1.44
B *Theocorythium trachelium*	NECC	20.8	21.3	1.76	1.80	1.78	5.35	6.85	1.30	1.59	1.44
B *Pterocorys minythorax*	NECC	14.75	15.25	1.24	1.28	1.26					
T *Pterocanium prismatium*	Sync	19.19	20.3	1.61	1.71	1.66	6.85	8.35	1.59	1.90	1.74
B *Anthocyrtidium angulare*	Sync	20.8	21.3	1.76	1.80	1.78	8.35	9.85	1.90	2.18	2.04
T *Lamprocyrtis heteroporos*	TROP	19.19	20.3	1.61	1.71	1.66	6.85	8.35	1.59	1.90	1.74
T *Anthocyrtidium jenghisi*	NEC	27.3	27.8	2.38	2.43	2.41					
B *Theocalyptra davisiana*	Sync	31.4	31.9	2.74	2.76	2.75					
T *Stichocorys peregrina*	SEC, NEC	31.9	32.4	2.76	2.81	2.79					
B *Lamprocyrtis neoheteroporos*	PC	36.31	36.4	3.14	3.18	3.16					
B *Lamprocyrtis heteroporos*	PC	36.4	36.9	3.14	3.18	3.16					
T *Anthocyrtidium pliocenica*	ED, PC	40.37	41.35	3.52	3.63	3.58					
B *Amphirhopalum ypsilon*	NECC	44.85	45.35	4.00	4.06	4.03					
T *Lychnodictyum audax*	TROP	42.15	42.47	3.76	3.78	3.77					
T *Phormostichoartus fistula*	NECC	39.82	40.37	3.46	3.52	3.49					
B *Spongaster tetras*	Sync*	45.85	46.35	4.12	4.18	4.15					
T *Didymocyrtis penultima*	Sync*	45.85	46.35	4.12	4.18	4.15					
T *Phormostichoartus doliolum*	SEC	42.85	44.35	3.81	3.95	3.88					
B *Pterocanium prismatium*	Sync*	50.34	57.45	4.49	4.98	4.74					
B *Theocorythium vetulum*	NECC	64.65	66.15	5.41	5.51	5.46					
T *Solenosphaera omnitubus*	TROP	57.45	58.95	4.98	5.08	5.03					
T *Siphostichartus corona*	SEC	72.21	75.25	5.90	6.06	5.98					
T *Stichocorys johnsoni*	TROP	78.75	79.24	6.24	6.28	6.26					
T *Calocycletta caepa*	SEC	85.92	86.5	6.77	6.80	6.78					
S. delmontensis > *S. peregrina*	TROP	87	87.5	6.80	6.84	6.82					
B *Solenosphaera omnitubus*	TROP	93.1	93.97	7.20	7.28	7.24					
T *Diartus hughesi*	Sync	98	98.5	7.62	7.66	7.64					
T *Botryostrobus miralestensis*	TROP	106	106.8	8.07	8.11	8.09					
T *Diartus petterssoni*	SEC	111	113	8.38	8.53	8.46					
D. petterssoni > *D. hughesi*	Sync	116.2	116.7	8.61	8.89	8.75					

TABLE 1e. (continued)

Events*	Types†	852 Depth (mcd)‡ Top	852 Depth (mcd)‡ Bottom	852 Age, Ma Top	852 Age, Ma Bottom	852 Md Age,§ Ma	853 Depth (mcd)‡ Top	853 Depth (mcd)‡ Bottom	853 Age, Ma Top	853 Age, Ma Bottom	853 Md Age,§ Ma
B *Stichocorys johnsoni*	NECC	116.73	117.2	8.97	9.11	9.04					
T *Stichocorys wolffii*	Sync	117.2	117.52	8.89	8.97	8.93					
T *Cyrtocapsella japonica*	Sync	121.7	122.72	9.95	10.05	10.00					
T *Carpocanopsis cristata*	NECC										

* T, last appearance; B, first appearance.

† "Type" denotes the Synchronous (Sync) and Diachronous events. An asterisk by the designation "Sync*" is given if the data from sites 844 and 845 are not considered in categorizing the event type. For the diachronous events the water mass or current system in which the first appearances appear the oldest and the last appearances appear the youngest are given under the heading "Type": ED, equatorial divergence; NEC, North Equatorial Current; NECC, North Equatorial Counter Current; PC, Peru Current extension; SEC, South Equatorial Current; Trop, Tropical water mass (north and south of the equatorial divergence - Peru Current extension).

‡ Here mcd is meters composite depth as used by Mayer et al. [1992].

§ The given median age is used (Figures 5-18).

TABLE 1f. Radiolarian Biostratigraphic Events, ODP Leg 138, Site 854 and Summary

Events*	Types†	854 Depth (mcd)‡ Top	854 Depth (mcd)‡ Bottom	854 Age, Ma Top	854 Age, Ma Bottom	854 Md Age,§ Ma	Summary Min	Summary Range‖	Summary Accu¶	Summary Age**
T *Stylatractus universus*	Sync	2.6	3.4	0.50	0.65	0.57	0.41	0.50	0.10	0.46
B *Collosphaera tuberosa*	Sync	2.6	3.4	0.50	0.65	0.57	0.58	0.65	0.06	0.61
T *Lamprocyrtis neoheteroporos*	Sync	4.1	5.6	0.78	1.03	0.91	1.02	1.12	0.10	1.07
T *Anthocyrtidium angulare*	Sync*	6.4	7.1	1.16	1.26	1.21	1.12(1.05)	1.25	0.13(0.20)	1.19
T *Theocorythium vetulum*	Sync	6.4	7.1	1.16	1.26	1.21	1.16	1.26	0.10	1.21
B *Lamprocyrtis nigriniae*	NEC	8.38	9.1	1.44	1.55	1.50	1.21	1.45	0.24	1.33
B *Theocorythium trachelium*	NECC	8.38	9.1	1.44	1.55	1.50	1.47	1.78	0.31	1.63
B *Pterocorys minythorax*	NECC	8.38	9.1	1.44	1.55	1.50	1.49	1.78	0.29	1.64
T *Pterocanium prismatium*	Sync	10.6	11.3	1.77	1.91	1.84	1.70	1.78	0.08	1.74
B *Anthocyrtidium angulare*	Sync	10.6	11.3	1.77	1.91	1.84	1.75	1.79	0.05	1.77
T *Lamprocyrtis heteroporos*	TROP	9.1	9.8	1.55	1.65	1.60	1.49	2.09	0.60	1.79
T *Anthocyrtidium jenghisi*	NEC	12.8	14.3	2.12	2.30	2.21	2.27	2.52	0.25	2.40
B *Theocalyptra davisiana*	Sync	15.8	16.6	2.49	2.59	2.54	2.65	2.76	0.11	2.71

TABLE 1f. (continued)

Events*	Types†	854					Summary			
		Depth (mcd)‡		Age, Ma		Md Age,§				
		Top	Bottom	Top	Bottom	Ma	Min	Range‖	Accu¶	Age**
T *Stichocorys peregrina*	SEC, NEC	15.8	16.6	2.49	2.59	2.54	2.49	2.88	0.39	2.69
B *Lamprocyrtis neoheteroporos*	PC	17.30	18.10	2.88	3.31	3.10	3.14	3.36	0.22	3.25
B *Lamprocyrtis heteroporos*	PC	17.30	18.10	2.88	3.31	3.10	3.14	3.44	0.30	3.29
T *Anthocyrtidium pliocenica*	ED, PC						3.13	3.63	0.50	3.38
B *Amphirhopalum ypsilon*	NECC						3.59	4.00	0.41	3.80
T *Lychnodictyum audax*	TROP						3.57	4.04	0.37	3.86
T *Phormostichoartus fistula*	NECC						3.48	5.30	1.82	4.39
B *Spongaster tetras*	Sync*						4.12(3.46)	4.23	0.11(0.77)	4.17
T *Didymocyrtis penultima*	Sync*						4.13	4.23(4.85)	0.09(0.72)	4.18
T *Phormostichoartus doliolum*	SEC						3.66	4.11	0.45	3.89
B *Pterocanium prismatium*	Sync*						4.72(3.46)	4.84	0.12(1.38)	4.78
B *Theocorythium vetulum*	NECC						4.87	5.45	0.58	5.16
T *Solenosphaera omnitubus*	TROP						4.98	5.81	0.83	5.40
T *Siphostichartus corona*	SEC						5.50	7.14	1.64	6.32
T *Stichocorys johnsoni*	TROP						6.24	6.48	0.24	6.36
T *Calocycletta caepa*	SEC						6.17	7.06	0.89	6.62
S. delmontensis > *S. peregrina*	TROP						6.56	6.81	0.25	6.69
B *Solenosphaera omnitubus*	TROP						6.97	7.28	0.31	7.13
T *Diartus hughesi*	Sync						7.62	7.72	0.10	7.67
T *Botryostrobus miralestensis*	TROP						8.07	8.59	0.52	8.33
T *Diartus petterssoni*	SEC						8.27	8.59	0.32	8.43
D. petterssoni > *D. hughesi*	Sync						8.59	8.72	0.13	8.66
B *Stichocorys johnsoni*	NECC						8.49	9.03	0.54	8.76
T *Stichocorys wolffii*	Sync						8.84	8.97	0.13	8.91
T *Cyrtocapsella japonica*	Sync						10.05	10.15	0.10	10.10
T *Carpocanopsis cristata*	NECC						10.37	10.84	0.47	10.61

* T, last appearance; B, first appearance.

† "Type" denotes the Synchronous (Sync) and Diachronous events. An asterisk by the designation "Sync*" is given if the data from sites 844 and 845 are not considered in categorizing the event type. For the diachronous events the water mass or current system in which the first appearances appear the oldest and the last appearances appear the youngest are given under the heading "Type": ED, equatorial divergence; NEC, North Equatorial Current; NECC, North Equatorial Counter Current; PC, Peru Current extension; SEC, South Equatorial Current; Trop, Tropical water mass (north and south of the equatorial divergence - Peru Current extension).

‡ Here mcd is meters composite depth as used by Mayer et al. [1992].

§ The given median age is used (Figures 5-18).

‖ The minimum range for each event is as defined in the text and Figure 1.

¶ The accuracy of each event is defined as the difference between the upper and lower bounds of the minimum range. It is used in plotting Figure 2.

** The age is taken as the midpoint of the minimum range and is used in plotting Figure 3.

mately 2-3 kyr in the leg 138 sites, and this upper part of the record is considered to have the more accurate time scale [Shackleton et al., 1993].

The tuned, 10-m.y.-long time scale is used to provide the age estimates for radiolarian events in sites 846-854. The tuned ages of paleomagnetic reversal datums and of the most reliable (i.e., synchronous) biostratigraphic datums (as determined in the other leg 138 sites for primarily calcareous nannofossils and diatoms), were applied to sites 844 and 845 where low carbonate concentrations in parts of the sections prevented the use of GRAPE stratigraphy. On the basis of age models thus constructed for these two sites, the ages of individual radiolarian events were determined by linear interpolation between the calibrated paleomagnetic and biostratigraphic datums.

The ages of the two samples which define each radiolarian event were plotted for each site and the "minimum age range" for the event within the study region was determined graphically (Figure 1). In this determination, the estimated minimum age range for each last occurrence event (T) is based on the age of the youngest sample in which the species appears that is consistent with the data from all the sites (lower boundary) and the oldest sample in which the species does not appear that is consistent with the data from all the sites (upper boundary). The estimated minimum age range for each first occurrence event (B) is based on the age of the youngest sample in which the species does not appear that is consistent with the data from all the sites (lower boundary) and the oldest sample in which the species appears that is consistent with the data from all the sites (upper boundary). These upper and lower bounds for the events define a minimum age range for each event studied in leg 138 sites. These plots were used to categorize individual events as being either synchronous (minimum age range $\leq$ 0.15 m.y.; Table 1) or diachronous (minimum age range > 0.15 m.y.)

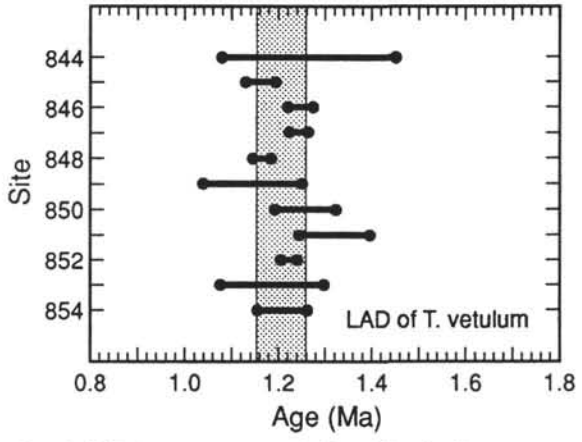

Fig. 1. Minimum range as defined for the last appearance datum (LAD) of *Theocorythium vetulum*. The lower bound is defined by sites 847 and 854 at 1.26 Ma (Table 1). This age is within or below the event range at all other sites studied. The upper bound is defined by site 854 at 1.16 Ma, which is within or above the event range at all other sites studied. The accuracy for this event, 0.10 m.y., is defined as the difference between the ages of the upper and lower boundaries of the minimum range.

The tuned time scale [Shackleton et al., 1993] provides a finely integrated chronostratigraphy for leg 138 sites. Although the absolute ages of the individual events will undoubtedly change with further refinement of this time scale, the relative age differences of diachronous events between individual sites should remain comparatively constant. In exploring the spatial pattern of these age differences, the average age of the upper and lower samples bounding the event is taken as the event age at each site (Table 1). The age difference in these bounding samples is usually less than 0.1 m.y. In the maps of individual first and last appearances (Figures 5 through 18) ages shown in brackets indicate that the resolution of the event at that site exceeds 0.1 m.y. (the contour interval). In such cases, contouring honors the observed range (Table 1), while remaining consistent with the more tightly constrained event ages at neighboring sites.

RESULTS

Definition of Synchrony

A minimum age range for 39 biostratigraphic events was determined for the 11 sites (844-854) which have a time scale that is either directly tuned to orbital parameters or is tightly linked to a tuned time scale that extends back to 10 Ma. All radiolarian events as determined in all sites are given in Table 1 along with the meters composite depth (mcd) of the samples used in the study [Moore, 1993]. The sampling program was designed to give resolution of 50-100 kyr in four key sites (845, 846, 848, and 852) representing the approximate geographic extremes of the study area. Of the seven remaining sites, four have average event ages that are less than 0.15 m.y. (Table 1). The remaining sites (844, 853, and 854) have, on average, more poorly constrained events. Such comparatively low resolution is usually a result of wide sample spacing [Moore, 1993].

A plot of the minimum age ranges for the nine tuned sites (sites 846-854; Figure 2a) show that the accuracy of these events vary from less than 50 kyr to approximately 1.8 million years. The median value for event accuracy is 0.29 m.y. There is a distinct break in the distribution of event accuracy at approximately 150 kyr. Thus an inter-site comparison of an event age that gives a minimum age range of 150 kyr or less seems like a reasonable choice for a working definition of the term "synchronous." This is approximately the same division between events that approach chronohorizons and those which are diachronous

events noted by Dowsett [1989]. A more detailed sampling scheme could well narrow the minimum age range for these events even further and place an even more stringent working definition on the concept of synchronous biostratigraphic events. There are 15 radiolarian events in the 9 "tuned " sites that meet this criteria.

The time scale for sites 844 and 845 are not directly tuned, but they are linked to that of sites 846-852 (see Methods section above and Shackleton et al. [1993]). When data from these two sites are included in the event accuracy plot (Figure 2b), the break in the distribution remains at approximately 0.15 m.y., and the median value for event accuracy of all 11 sites is 0.31 m.y. Clearly, the inclusion of these two northeastern sites only slightly decreases the average accuracy of radiolarian events in leg 138 data set. When we consider the entire data set, only 11 radiolarian events meet the 0.15 m.y. cutoff for synchrony.

It is not known whether this slight decrease in event accuracy is a result of a more imprecise time scale for the two northeastern sites or a result of a real tendency for increased diachrony when sites from the easternmost parts of the North Equatorial Counter Current, Costa Rica Dome, and North Equatorial Current are included in the data set. It is probable that both factors have an effect; however, of the four events which have markedly different ages in the northeastern sites, three occur in the rather narrow time range of approximately 3.5 to 5.0 Ma. This region is expected to have undergone significant oceanographic change at approximately this time as the Isthmus of Panama closed; thus the apparent diachrony of these radiolarian events may indeed be real. As we show later, several diachronous events of approximately this age have marked differences between their ages in these northeastern sites and those further to the west.

A plot of radiolarian events versus median age of each event at all sites (Figure 3) indicates that there tends to be a larger number of synchronous events (in both relative and absolute numbers) in the last two million years than in earlier times. It might be proposed that the nature of climatic and oceanographic change associated with northern hemisphere glaciations could have favored a larger number of synchronous first and last appearances; while the nature of oceanographic variation between approximately 4 and 6 Ma favored diachronous first and last appearances. Two factors should be remembered, however, that argue against making too much of the temporal pattern of biostratigraphic events shown in Figure 3. First, the selection of species used in this study was neither random nor complete [Moore, 1993]; thus the pattern shown might be highly biased by the process of species selection. Second, a great deal more work has been done on the stratigraphy of the last few million years than on earlier intervals. This is the part of the section within the reach of normal piston cores. Researchers have a much clearer

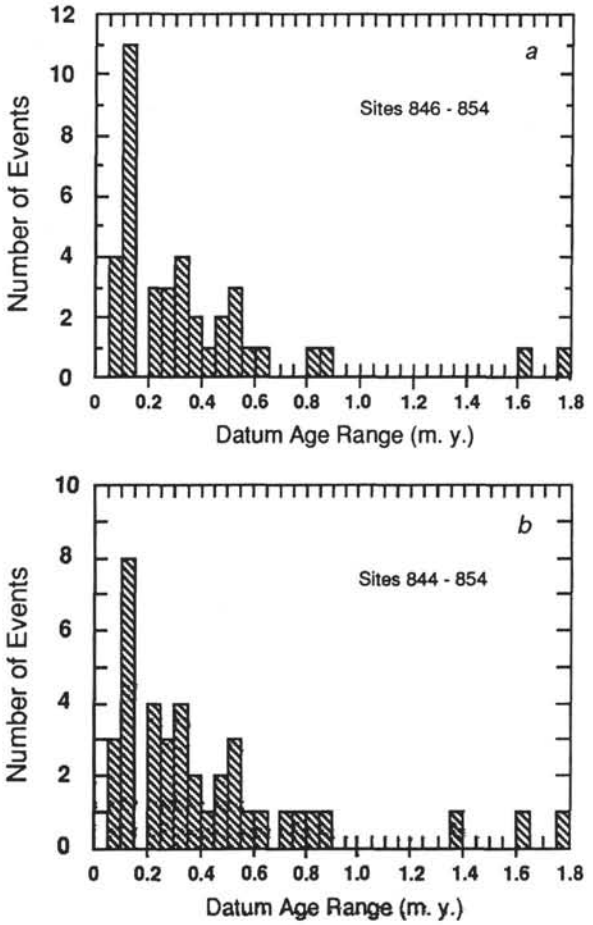

Fig. 2. (a) The distribution of event accuracy (as defined in the text and Figure 1) for 39 radiolarian events in the orbitally tuned sites 846-854. (b) The distribution of event accuracy for 39 radiolarian events in all sites studied (data from Table 1).

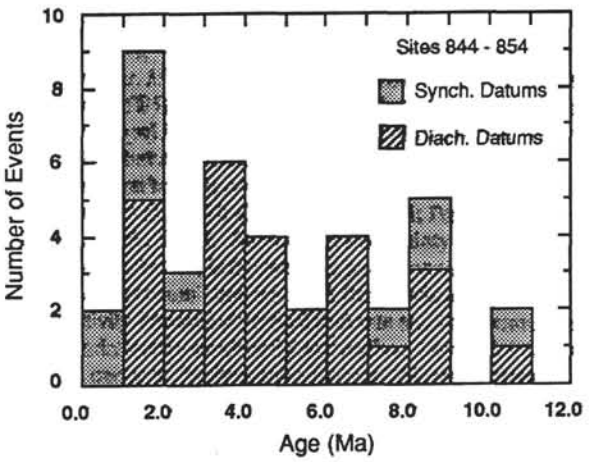

Fig. 3. The distribution of synchronous and diachronous radiolarian events as a function of age (data from Table 1).

picture of radiolarian stratigraphy for this interval, and we may have selected against those events which are clearly diachronous. Given these caveats, it appears that prior to 2 Ma, the number of synchronous events is usually no more than approximately one per million years. The events are not evenly distributed with time. There may tend to be a greater number of events at times of major oceanographic change, such as the onset of northern hemisphere glaciation (approximately 2 Ma), and the time following the rapid decrease in equatorial biogenic deposition rates (3-4 Ma [Shackleton et al., 1992]).

Patterns of Diachrony

It is generally thought that a new species forms in a genetically isolated enclave. Once established it can migrate out of its "home" region by adapting to different environmental conditions, by outcompeting species in other regions, or by taken advantage of changing environmental conditions to expand its range. Conversely, changing environmental conditions or increased competition can cause a decrease in the geographic range of a species and lead to a sudden or a gradual extinction.

It has been amply demonstrated that the zoogeography of most modern planktonic species (including radiolarians) match the distribution of surface water masses and current systems [e.g., Morley, 1989a, b; Pisias, 1986; Lombari and Boden, 1985; Moore, 1978; Molina-Cruz, 1977]. It seems logical to propose that the gene pool of such planktonic species is circumscribed by the water masses and current systems in which they live. Currents, oceanic fronts, and the vertical structure of the oceans do not form totally impermeable boundaries to the migration of species; however, the sharpness of the oceanographic gradients (either vertical or horizontal) in the waters surrounding the habitat of individual species is some measure of the difficulty a species might encounter in expanding (or maintaining) its range. Changes in climatic and oceanographic conditions, changes in current patterns and vertical structure of the oceans, and changes in the lateral boundaries of the ocean basins could be expected to spur evolution, migration, and extinction of planktonic species through the impact of these changes on the planktonic gene pools.

The eastern equatorial Pacific area sampled by the leg 138 sites is only slightly smaller than the equatorial Atlantic Ocean. It is an area with a very complex circulation pattern, strong vertical and horizontal oceanic gradients, and marked differences in primary productivity (Figure 4). For those radiolarian species which show diachronous first or last appearances in leg 138 sites, the spatial and temporal patterns of these biostratigraphic events may be linked to the circulation patterns of the surface and near surface currents. If this is true, then the temporal patterns of occurrence of these events when seen in map view may indeed monitor the evolution of ocean circulation and structure in this region.

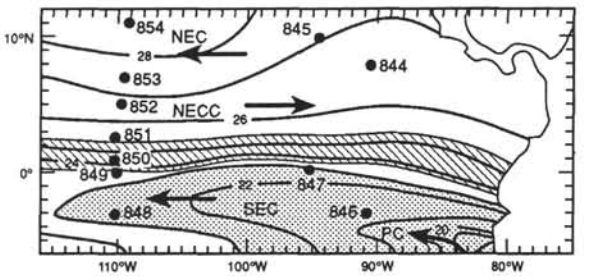

Fig. 4. Site locations for ODP leg 138 shown on a map of modern August sea surface temperature (contours in degrees Celsius). The zonal region of high thermal gradient at the southern boundary of the North Equatorial Counter Current is shaded and shown on Figures 5-18 as a reference. PC, Peru Current; SEC, South Equatorial Current; NEC, North Equatorial Current; NECC, North Equatorial Counter Current. Arrows indicate direction of current flow.

In order to investigate this possibility, the average age of the diachronous biostratigraphic events at each site are plotted and contoured in Figures 5 through 18. The position of these sites have been rotated according to the plate rotation scheme of Cox and Engebretson [1985]. Taking into account the resolution of the event ages, they are contoured at 0.1 m.y. intervals to show the spatial and temporal patterns formed by the expansion (first appearances) and contraction (last appearances) of the geographic ranges of each species. Areas are shaded with crosshatching to indicate the region of youngest last occurrence and with diagonal shading in regions of oldest first occurrence. The zonal band of stippling in each figure denotes the position of high thermal gradient in the modern ocean (from Figure 4).

There are several general aspects of these maps to note. With very few exceptions the patterns in time and space seem to indicate that each species is originally (oldest first occurrence) or ultimately (youngest last occurrence) associated with a particular water mass or current system. Over a period of several hundred thousand years it appears that the species either expanded their range (from its area of oldest first occurrence) or withdrew into a refuge (to its area of youngest last occurrence) before disappearing from the region altogether. In both cases there are particular areas or zones where the difference in event ages between control points (sites) is high; thus it took a longer period of time for the range of the species to cross the region that separates these sites. By comparing the temporal patterns of the events younger than approximately 3 Ma (Figures 5-9) to the map of modern sea surface temperature (Figure 4) and to other known oceanographic features of the modern circulation patterns, it can be seen that the regions with high temporal gradients in these event maps closely correspond to regions of high oceanographic gradients. Thus the oceanographic boundaries do appear to serve as at least temporary

barriers to changes in the geographic ranges of the species. On the basis of this observation, we can now go back in time and use the spatial-temporal patterns of extinctions and first appearances as a guide to how and when oceanographic boundaries may have changed their positions.

Figures 5-18 are arranged in chronologic order of the event age (youngest to oldest) and show approximately half of the diachronous events listed in Table 1. Although all of the diachronous events studied show coherent regional patterns of timing of the first and last appearances, a few appear to show errors in identification or timing at a particular site. The events illustrated and discussed below show very clear associations with particular current systems.

Lamprocyrtis nigriniae (Figure 5) first appeared in the region of the North Equatorial Current (NEC). A region of high temporal gradient was at approximately 6°-7° N, near the southern boundary of the NEC. There is a slight indication that the high productivity region of the equatorial divergence was the last area to be invaded by this species.

Theocorythium trachelium (Figure 6) first appeared in the North Equatorial Counter Current (NECC) and had high temporal gradients between 1° and 3° N and 6° and 7° N.

Anthocyrtidium jenghisi (Figure 7) had its youngest last occurrence in the region of the NEC. Much like *Lamprocyrtis nigriniae,* which first appeared in the NEC approximately 0.7 m.y. later, *A. jenghisi* did not seem to fare well in the narrow equatorial divergence. It disappeared from this region first. There does not appear to have been a high gradient area for this event; however, data for this (and older) events are lacking from site 853 (at approximately 7° N).

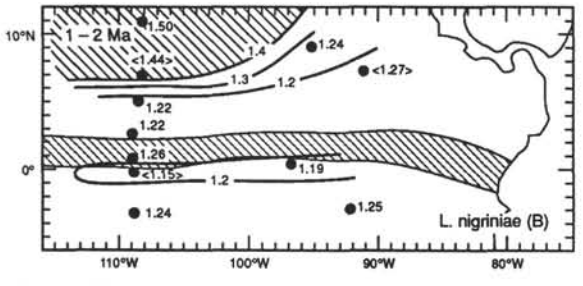

Fig. 5. Timing of the first occurrence event of *Lamprocyrtis nigriniae.* Diagonally shaded area indicates region of earliest first occurrence. Contour interval is 0.1 m.y. ODP leg 138 site positions as determined by the rotations given by Cox and Engebretson [1985]. Numbers at each site give the median age of the event at that site (from Table 1). Numbers in brackets indicate events with a range of estimate greater than 0.1 m.y. Open symbols are shown at site locations where the event was not defined. The irregular zone of stippled shading indicates the region of high thermal gradient found in modern August sea surface temperatures.

Anthocyrtidium pliocenica (Figure 8), by contrast, last appeared in the equatorial divergence area and the westward extension of the Peru Current (PC). It apparently thrived best in this region of high productivity and had sharp temporal gradients in its last occurrence to both the north and south of the equator.

Lamprocyrtis heteroporos (Figure 9) also appears to have done well in cooler, high productivity waters and to have entered the tropical Pacific via the PC. Note that the region of high temporal gradient for this event seems to match well the region of high thermal gradient in the modern ocean (Figure 4).

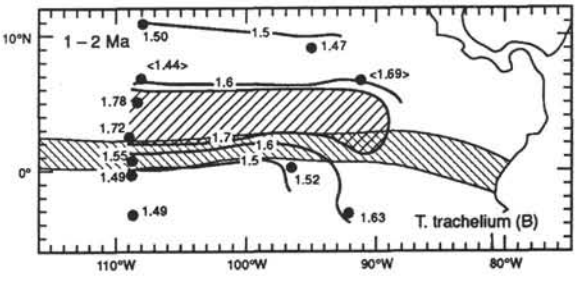

Fig. 6. Timing of the first occurrence event of *Theocorythium trachelium.* Diagonally shaded area indicates region of earliest first occurrence. Other conventions are as in Figure 5.

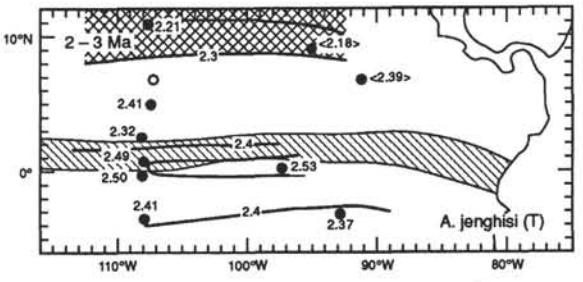

Fig. 7. Timing of the last occurrence event of *Anthocyrtidium jenghisi.* Cross-hatched shaded area indicates region of latest last occurrence. Other conventions are as in Figure 5.

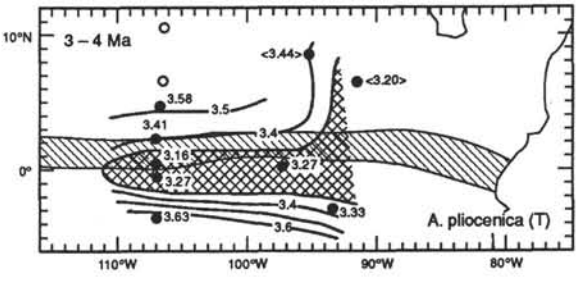

Fig. 8. Timing of the last occurrence event of *Anthocyrtidium pliocenica.* Cross-hatched shaded area indicates region of latest last occurrence. Other conventions are as in Figure 5.

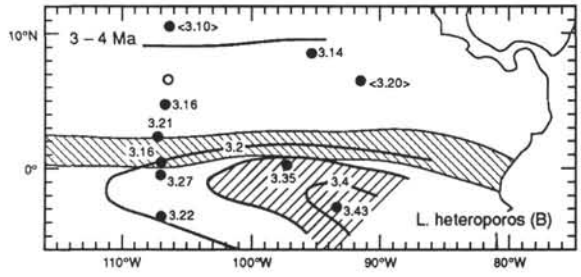

Fig. 9. Timing of the first occurrence event of *Lamprocyrtis heteroporos*. Diagonally shaded area indicates region of earliest first occurrence. Other conventions are as in Figure 5.

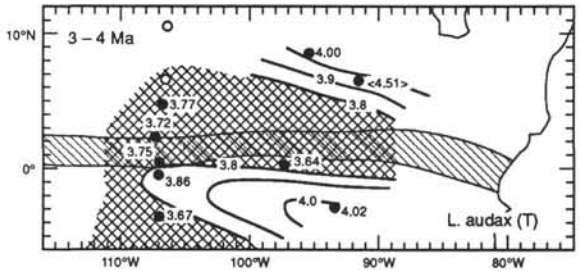

Fig. 10. Timing of the last occurrence event of *Lychnodictyum audax*. Cross-hatched shaded area indicates region of latest last occurrence. Other conventions are as in Figure 5.

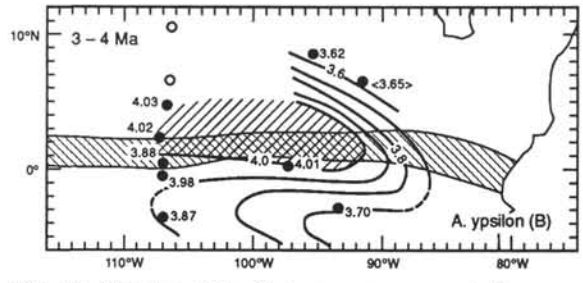

Fig. 11. Timing of the first occurrence event of *Amphirhopalum ypsilon*. Diagonally shaded area indicates region of earliest first occurrence. Other conventions are as in Figure 5.

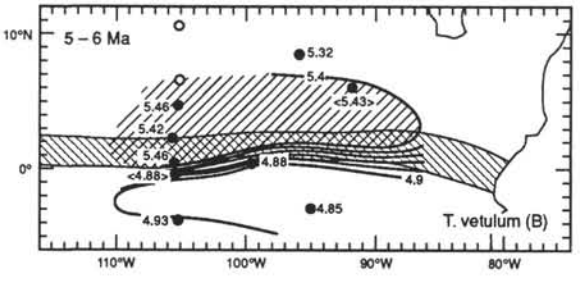

Fig. 12. Timing of the first occurrence event of *Theocorythium vetulum*. Diagonally shaded area indicates region of earliest first occurrence. Other conventions are as in Figure 5.

Lychnodictyum audax (Figure 10) shows a somewhat different pattern. It had its youngest last occurrence in the NECC and in the warmer waters of the SEC, but there was a subtle difference in the position of the areas of high temporal gradient. The southern bound of this NECC-associated distribution appears to have been shifted 1° or 2° to the south. There is also a distinct difference between the event ages of the sites on the northern part of the western transect (850-852) and those in the northeast (844 and 845), suggesting the existence of a high oceanographic gradient between these two areas that is not seen in the maps of younger events.

Amphirhopalum ypsilon (Figure 11), whose first occurrence event is also associated with the NECC, shows a very similar pattern to that of the slightly younger last occurrence of *Lychnodictyum audax* - a slight southward shift in the southern boundary of the NECC-associated distribution and the development of a high temporal gradient region in the northeastern part of the study area.

Theocorythium vetulum (Figure 12) also first appeared in the area of the NECC. It has an extremely sharp temporal gradient (approximately 0.6 m.y.) at its southern bound which is slightly south of the modern area of high thermal gradient. The taxonomy of this species is not well studied in the youngest part of its range; thus the exact pattern presented here may change with further taxonomic work.

Solenosphaera omnitubus (Figure 13) is another tropical species which does not appear to have fared well in the equatorial divergence area. It disappeared first from this area and from the sites located in the more productive, easternmost part of the tropical Pacific. The first occurrence of this species (7.1-7.4 Ma) showed a nearly identical temporal pattern, appearing last in the area of equatorial divergence.

Siphostichartus corona (Figure 14) became very rare in the upper part of its range; thus, we might expect that its last appearance would fail to show a clear pattern. It does, however, show a fairly simple picture. It survived longer in the SEC; and there was a sharp temporal gradient at the northern bound of this current, which appears to have been slightly south of

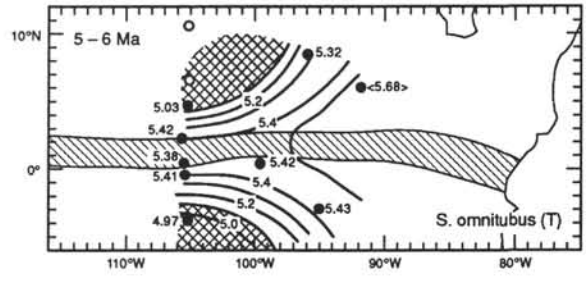

Fig. 13. Timing of the last occurrence event of *Solenosphaera omnitubus*. Cross-hatched shaded area indicates region of latest last occurrence. Other conventions are as in Figure 5.

the modern high gradient area. There is also a fairly large age difference (up to 1 m.y.) in the last appearance of this species between the two northeastern transect sites.

Stichocorys johnsoni (Figure 15) disappeared first from what were presumably the cooler, more productive waters of the PC and the eastern tropical Pacific. The high gradient zone between the northeastern and western sites was still present as was the one at approximately 0°-2°N.

Botryostrobus miralestensis (Figure 16) persisted longest in the NEC and in the southern part of the SEC. This pattern suggests the negative influence of the PC extension and/or the equatorial divergence zone, but there are important differences between this pattern and the ones seen after approximately 6 Ma. First, there was the development of a strong gradient between the southernmost sites and those directly to the north; and second, the strong temporal gradient in the northeastern part of the area appears to have been weaker and more zonal in nature.

Diartus petterssoni (Figure 17) persisted longest in a rather broad equatorial zone with sharp zonal gradients to the north and south. The areas of high gradient to the south and between sites 844 and 845 were similar in position to that seen for *Botryostrobus miralestensis* (Figure 16).

Stichocorys johnsoni (Figure 18) appeared first in the area of the NECC in a temporal pattern that is similar to that of its last appearance (Figure 15). There are differences, however, in the position and orientation of the high gradient regions. They were more zonal and a bit further south for the first occurrence of the species. There was also a steep southern gradient similar to that found for *Botryostrobus miralestensis* (Figure 16) and *Diartus petterssoni* (Figure 17).

DISCUSSION

The study area is probably too small to make a claim that any of the species studied formed locally in a particular water mass, but it does appear that within this region approximately one quarter of the 28

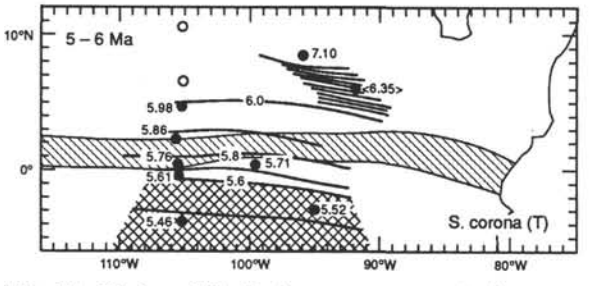

Fig. 14. Timing of the last occurrence event of *Siphostichartus corona*. Cross-hatched shaded area indicates region of latest last occurrence. Other conventions are as in Figure 5.

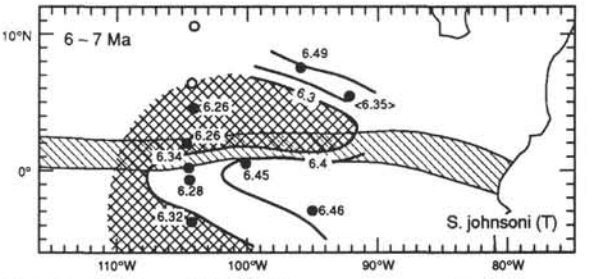

Fig. 15. Timing of the last occurrence event of *Stichocorys johnsoni*. Cross-hatched shaded area indicates region of latest last occurrence. Other conventions are as in Figure 5.

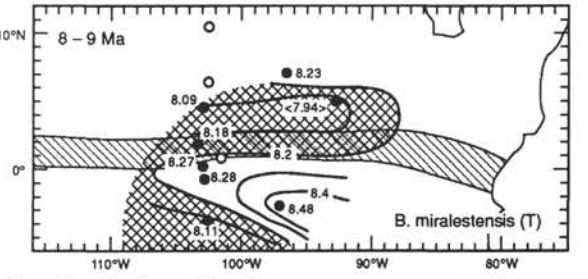

Fig. 16. Timing of the last occurrence event of *Botryostrobus miralestensis*. Cross-hatched shaded area indicates region of latest last occurrence. Other conventions are as in Figure 5.

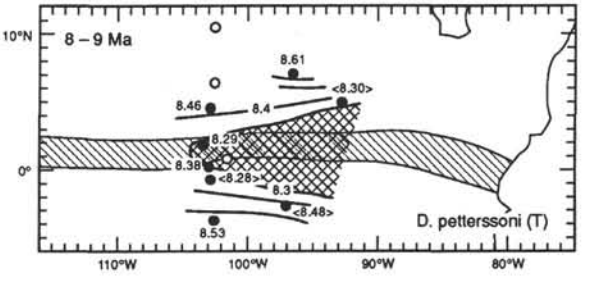

Fig. 17. Timing of the last occurrence event of *Diartus petterssoni*. Cross-hatched shaded area indicates region of latest last occurrence. Other conventions are as in Figure 5.

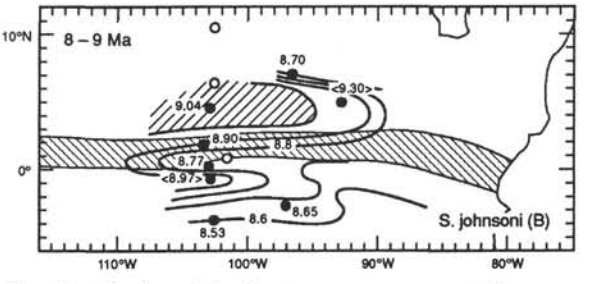

Fig. 18. Timing of the first occurrence event of *Stichocorys johnsoni*. Diagonally shaded area indicates region of earliest first occurrence. Other conventions are as in Figure 5.

diachronous events studied are associated with earliest first occurrence (5) or latest last occurrence (2) in the area of the NECC (Table 1). There are also seven events which have their earliest first occurrence or latest last occurrence in regions north and south of the equator (outside the PC extension and equatorial divergence zone). Most of these are oldest last occurrences. Only two closely related species apparently emigrated into the area via the PC, *Lamprocyrtis heteroporos* and *L. neoheteroporos*. Only one other (*Anthocyrtidium pliocenica*) is closely linked with the equatorial zone of divergence and high productivity.

There are nearly twice as many last occurrences as first occurrences considered (Table 1) in this study, but there does not seem to be any strong difference in the rapidity of these two types of events. The average progression of extinction through the study area (Md = 0.37 m.y.) is only slightly longer than the average period of invasion (Md = 0.26 m.y.). Thus it seems to take on the order of 300 kyr for a species to invade this oceanographically complex region and establish itself throughout the area. Similarly, it takes approximately the same amount of time (perhaps a little longer) for a species to disappear from the region. This argues for a somewhat similar process effecting these population changes. Perhaps this span of time is a measure of how long it takes inter-specific competition, interacting with the natural variability of oceanographic conditions, to have an effect. Perhaps it is a measure of mutation or adaptation rates. Or perhaps it is an indication that planktonic species always fare best in a particular oceanic region, and as long as they are doing well in that region, they can continuously provide emigrant stock for the population of surrounding areas, areas in which the species does not fare quite as well. When they are first becoming established and when they start to do less well in their home area, they are less able to supply this stock of invaders. At these times their geographic range takes a few 100 kyr to expand (for first appearances) or contract (for last appearances). Further quantitative study is needed to address these speculations.

It may well be that even the radiolarian species defined as having synchronous events in this study have patterns of first and last occurrence that are similarly coherent in map view. Preliminary maps of some synchronous events seem to indicate coherent patterns taking place over a shorter period of time. This aspect of the study awaits a further refinement of the time scales for the leg 138 sites and a closer spacing of biostratigraphic samples.

The patterns of extinction and first occurrence revealed by the diachronous radiolarian events seem to give some hint as to both the timing and character of circulation changes occurring in the eastern tropical Pacific over the past 10 Ma. In the older part of the record there are strong zonal gradients in the temporal patterns of first and last appearance events at approximately 2°-3°S and at approximately 6°-7°N. The southern boundary may reflect the influence of the equatorial divergence; however, the patterns of both *Botryostrobus miralestensis* (Figure 16) and *Diartus petterssoni* (Figure 17) seem to indicate a fairly broad region of the normally cool, nutrient-rich equatorial waters, extending from approximately 2°-3°S to 3°-4°N. If these high gradient zones represents the bounds of the SEC, then it was shifted somewhat north of its present position. The sharp gradient at approximately 1°N shown by the first appearance of *Stichocorys johnsoni* may indicate the influence of the equatorial divergence itself on this species.

The pattern of the last appearance *Stichocorys johnsoni* (Figure 15) that occurred at 6 to 7 Ma is markedly different from those that occurred before this time. It indicates that the cool PC waters extended up to only approximately 1°N and that there was a less zonal character in the temporal gradient to the north. The time period covered by this event represents an interval of rapid increase in biogenic sediment accumulation rates [Shackleton et al., 1992]. It is not clear how these suggested shifts in the circulation patterns might have affected the flux of biogenic sediments in the region, but the coincidence in the timing of these changes is very close.

All the events from approximately 6 Ma to approximately 3.7 Ma (an interval of relatively high accumulation rates throughout most of the study region) show a very similar and consistent pattern: (1) a zone of high temporal gradients at approximately 0°-1°N (one or two degrees south of the present-day zone of high thermal gradient) and (2) a relatively steep temporal gradient between the northeastern sites and the northern sites of the western transect. This pattern suggests that the southern boundary of the NECC was south of its modern position and that there was a fairly strong oceanic gradient between the NECC coming from the west and the NEC. The NEC may have been augmented by flow from the Caribbean during this time, but the gradual closure of the Isthmus may have deflected flow somewhat to the south and set up the strong gradients found between the northern sites of the eastern and western transect.

There is a subtle, but recognizable change in this pattern occurring between the last appearance of *Lychnodictyum audax* (3.7-4.0 Ma, Figure 10) and the first appearance of *Lamprocyrtis heteroporos* (3.1-3.4 Ma, Figure 9). The southern bound of the NECC apparently shifted northward to its modern position and the the strong gradients between the northern sites of the eastern and western transects largely disappeared. The nature of these changes together with the coincidence of their timing with the closing of the Isthmus of Panama strongly suggests that the shut off of the connection between the Caribbean and the Pacific reduced the strength of the NEC, reduced the sharp oceanic gradient between the northeastern and northwestern sites, and caused the NECC/SEC boundary to be shifted slightly to the north.

The patterns of occurrence shown for events younger than approximately 3 Ma are consistent with modern circulation patterns.

CONCLUSIONS

The need for biostratigraphers to provide a guide to paleomagnetists will always be present. By working with paleomagnetists, biostratigraphers can establish which of their events are approximately synchronous. Results of our studies of the ODP leg 138 sites indicate that according to our working definition of "synchronous," approximately one third to one fourth of the radiolarian events investigated occur at approximately the same time throughout the study area. Closer sample spacing and the continued refinement of the time scale may reduce this number by allowing us to make a more stringent working definition of the synchronous category. The median diachrony for all events in this study is approximately 0.3 m.y. This average degree of accuracy is only slightly less than what is generally taken as the accuracy of chronostratigraphies based solely on biostratigraphic events.

With their approximately synchronous events, biostratigraphers also help those scientists who attempt to tune the more continuous, quantitative stratigraphies to the calculated orbital time scale. Given an orbitally tuned time scale for a suite of sites, however, biostratigraphers have an opportunity to go far beyond the traditional limits of their science. No longer should we cast aside a particular biostratigraphic event simply because it appears to be diachronous. The very nature of that diachrony, when placed in the context of a well-established chronostratigraphy and a well-defined taxonomy, gives clues to the processes by which evolution, migration, and extinction of species occur. Furthermore, the temporal-spatial pattern of that diachrony can be tied to ocean circulation patterns. By investigating a whole series of diachronous biostratigraphic events they can provide important information on how circulation patterns changed with time.

The diachronous events that occur in leg 138 sites over the last 3 Ma show a close correspondence between their temporal-spatial patterns of first and last appearances and the modern oceanographic patterns of temperature, productivity and near-surface circulation. On the basis of this observation, we have used similar patterns of extinction and first occurrence to deduce the nature of circulation changes in the eastern tropical Pacific over the past 10 Ma.

Prior to approximately 7 Ma, the strong zonal gradients at approximately 2°-3°N and 3°-4°S suggest that the SEC may have been slightly north of its present position. There was a marked change in this pattern between 6 and 7 Ma. At this time the western extension of the Peru Current appeared to have been at or just north of the equator and there was an increase in the gradient between the northeastern and northwestern sites. This marks the time of a substantial increase in the accumulation rate of biogenic sediments in the tropical Pacific as well as in other regions of the oceans.

From approximately 6 to 3.7 Ma the relatively high gradients between the northern sites of the eastern and western transects remained, suggesting a strong contrast between the waters of the NECC and those of the NEC, which may have been augmented by flow from the Caribbean. This change in pattern may reflect a deflection of the flow through the Isthmus as it gradually closed. The southern boundary of the NECC remained just south of its present position.

Diachronous events younger than approximately 3.4 Ma show temporal spatial patterns that are consistent with modern near-surface circulation patterns. The apparent circulation change at approximately 3.4-3.7 Ma is thought to have occurred as a result of the closing of the Isthmus of Panama.

Acknowledgments. We thank the scientists, technical staff, and ship's personnel of ODP leg 138, whose efforts made this study possible. We particularly thank the stratigraphers who worked so hard to put together the accurate composite sections. This research was supported in part by grants to TCM and NGP from the U. S. Science Support Program to the Ocean Drilling Program, and to N.J.S. from the NERC Ocean Drilling Program Special Topic Research grant GST/02/554.

REFERENCES

Alexandrovich, J. M., Stratigraphy, sedimentology, and paleoceanography of the eastern equatorial Pacific: Late Miocene through Pleistocene, Doctoral dissertation, 435 pp., Columbia Univ., Palisades, N.Y., 1992.

Berger, A., and M. F. Loutre, Insolation values for the climate of the last 10 million years, *Quat. Sci. Rev., 10*, 297-317, 1991.

Berggren, W. A., J. D. Phillips, A. Bertrels, and D. Wall, Late Pliocene-Pleistocene stratigraphy in deep-sea cores from the south-central North Atlantic, *Nature, 216,* 253-254, 1967.

Cande, S. C., and D. V. Kent, A new geomagnetic polarity time scale for the Late Cretaceous and Cenozoic, *J. Geophys. Res., 97*(B10), 13,917-13,952, 1992.

Caulet, J.-P., C. Nigrini, and D. A. Schneider, High resolution Pliocene-Pleistocene radiolarian stratigraphy of the tropical Indian Ocean, *Mar. Micropaleontol.*, in press, 1993.

Cox, A., and D. Engebretson, Changes in motion of Pacific plate at 5 Myr BP, *Nature, 313,* 472-474, 1985.

Dowsett, H. J., Diachrony of late Neogene microfossils in the southwest Pacific Ocean: Application of the graphic correlation method, *Paleoceanography, 3*(2), 209-222, 1988.

Dowsett, H. J., Application of the graphic correlation method to the Pliocene marine sequences, *Mar. Micropaleontol., 14*, 3-32, 1989.

Hagelberg, T., et al., Development of the composite depth sections for sites 844 through 854, in *Proceedings of the Ocean Drilling Program, Initial*

Reports, vol. 138, edited by L. Mayer et al., pp. 79-86, Ocean Drilling Program, College Station, Tex., 1992.

Hays, J. D., Stratigraphy and evolutionary trends of radiolaria in North Pacific deep-sea sediments, in Geological Investigations of the North Pacific, *Geol. Soc. Am. Mem., 126,* 185-218, 1970.

Hays, J. D., Faunal extinctions and reversals in the Earth's magnetic field, *Geol. Soc. Am. Bull., 82,* 2433-2447, 1971.

Hays, J. D., and N. J. Shackleton, Globally synchronous extinction of the radiolarian *Stylatractus universus, Geology, 4*(11), 649-652, 1976.

Hays, J. D., T. Saito, N. D. Opdyke, and L. H. Burckle, Pliocene-Pleistocene sediments of the equatorial Pacific - Their paleomagnetic, biostratigraphic and climatic record, *Geol. Soc. Am. Bull., 80,* 1481-1514, 1969.

Johnson, D. A., and A. H. Knoll, Absolute ages of Quaternary radiolarian datum levels in the equatorial Pacific, *Quat. Res., 5,* 99-110, 1975.

Johnson D. A., and C. A. Nigrini, Synchronous and time-transgressive Neogene radiolarian datum levels in the equatorial Indian and Pacific Oceans, *Mar. Micropaleontol., 14,* 33-36, 1985.

Johnson, D. A., and B. J. Wick, Precision of radiolarian datum levels in the middle Miocene, equatorial Pacific, *Micropaleontology, 28*(1), 43-58, 1982.

Johnson, D. A., D. A. Schneider, C. A. Nigrini, J. P. Caulet, and D. Kent, Pliocene-Pleistocene radiolarian events and magnetostratigraphic calibrations for the tropical Indian Ocean, *Mar. Micropaleontol., 14,* 33-66, 1989.

Kennett, J. P., Pleistocene paleoclimates and foraminiferal biostratigraphy in subantarctic deep-sea cores, *Deep Sea Res., 17,* 125-140, 1970.

Kennett, J. P., The development of planktonic biogeography in the southern ocean during the Cenozoic, *Mar. Micropaleontol., 3,* 301-345, 1978.

Lombari, G., and G. Boden, Modern radiolarian global distributions, *Cushman Found. Foraminiferal Res. Spec. Publ., 16A,* 125 pp., 1985.

Mayer, L., et al., *Proceedings of Ocean Drilling Program, Initial Reports,* vol. 138, 1462 pp., Ocean Drilling Program, College Station, Tex., 1992.

Molina-Cruz, A., Radiolarian assemblages and their relationship to the oceanography of the subtropical southeastern Pacific, *Mar. Micropaleontol., 2,* 315-352, 1977.

Moore, T.C., Jr., The distribution of radiolarian assemblages in the modern and ice-age Pacific, *Mar. Micropaleontol., 3,* 229-266, 1978.

Moore, T. C., Jr., Radiolarian stratigraphy, ODP Leg 138, in *Proceedings of Ocean Drilling Program, Scientific Results,* vol. 138, edited by L. Mayer et al., Ocean Drilling Program, College Station, TX, in press, 1993.

Morley, J. J., Variations in high-latitude oceanographic fronts in the southern Indian Ocean: An estimation of faunal changes, *Paleoceanography, 4*(5), 547-554, 1989a.

Morley, J. J., Radiolarian-based transfer functions for estimating paleoceanographic conditions in the south Indian Ocean, *Mar. Micropaleontol., 13*(4), 293-308, 1989b.

Pisias, N. G., Vertical water mass circulation and the distribution of radiolaria in surface sediments of the Gulf of California, *Mar. Micropaleontol., 10,* 189-205, 1986.

Shackleton, N., et al., Sedimentation rates: toward a GRAPE density stratigraphy for leg 138 carbonate sections, in *Proceedings of Ocean Drilling Program, Scientific Results,* vol. 138, edited by L. Mayer et al., pp. 87-92, Ocean Drilling Program, College Station, Tex., 1992.

Shackleton, N. J., S. Crowhurst, T. Hagelberg, N. Pisias, and D. A. Schneider, A new late Neogene time scale: Application to ODP leg 138 sites, in *Proceedings of Ocean Drilling Program, Scientific Results,* vol. 138, edited by L. Mayer et al., Ocean Drilling Program, College Station, Tex., in press, 1993.

Theyer, F., C. Y. Mato, and S. R. Hammond, Paleomagnetic and geochronologic calibration of latest Oligocene to Pliocene radiolarian events, equatorial Pacific, *Mar. Micropaleontol., 3,* 377-395, 1978.

T. C. Moore, Jr., Department of Geological Sciences, University of Michigan, Ann Arbor, MI 48109-1063.

N. G. Pisias, College of Oceanography, Oregon State University, Corvallis, OR 97331-5503.

N. J. Shackleton, Subdepartment of Quaternary Research, University of Cambridge, Cambridge CB2 3RS, United Kingdom.

(Received February 17, 1993;
revised May 18, 1993;
accepted May 19, 1993.)